Acta Materialia 111 (2016) 187–193

Contents lists available at ScienceDirect

Acta Materialia

journal homepage: www.elsevier.com/locate/actamat

Full length article

# Mapping of residual strains around a shear band in bulk metallic glass by nanobeam X-ray diffraction

Hamed Shakur Shahabi [a, b, *], Sergio Scudino [a], Ivan Kaban [a, b], Mihai Stoica [a, c], Benjamin Escher [a, b], Siegfried Menzel [a], Gavin B.M. Vaughan [d], Uta Kühn [a], Jürgen Eckert [e, f]

[a] IFW Dresden, Institute for Complex Materials, P.O. Box 27 01 16, D-01171 Dresden, Germany
[b] TU Dresden, Institut für Werkstoffwissenschaft, D-01062 Dresden, Germany
[c] Politehnica University Timisoara, P-ta Victoriei 2, RO-300006 Timisoara, Romania
[d] European Synchrotron Radiation Facilities ESRF, BP 220, 38043 Grenoble, France
[e] Erich Schmid Institute of Materials Science, Austrian Academy of Sciences, Jahnstraße 12, A-8700 Leoben, Austria
[f] Department Materials Physics, Montanuniversität Leoben, Jahnstraße 12, A-8700 Leoben, Austria

ARTICLE INFO

*Article history:*
Received 20 January 2016
Received in revised form
11 March 2016
Accepted 11 March 2016

*Keywords:*
Bulk metallic glass
X-ray diffraction
Shear band
Atomic structure
Pair distribution function

ABSTRACT

Despite recent progress in understanding the outstanding role of shear bands in plastic deformation of metallic glasses, the details of structural changes in the shear-induced zone is not yet known. In order to probe such changes, we determined the distribution of residual strains at short- and medium-range order around a single shear band in cold-rolled Vit105 bulk metallic glass using a nano-focused high energy X-ray beam. Plastic deformation results in significant residual normal and shear strains at distances of more than 15 μm around the shear band. Based on a detailed analysis of the distribution profile, the magnitude and the direction of the residual shear strain, it is suggested that the shear strain plays a dominant role, compared to the normal strains, for triggering nucleation of further shear bands from a mature shear band.



## 1. Introduction

Shear banding is known as the main mechanism of plastic deformation in metallic glasses at ambient temperature. A shear band is a very thin (10–20 nm) localized sheared region which nucleates by cooperative action of numerous shear transformation zones (STZs) formed by sliding of energetically favored atomic clusters under shear stress [1,2]. The overall plastic deformation behavior of bulk metallic glasses (BMGs) at ambient temperature is a consequence of several characteristics of shear bands including the number, distance, direction, temperature, shear offset, propagation speed and their mutual interactions [1–3]. This outstanding role of shear bands has appealed almost all attempts aiming to resolve the biggest Achilles heel of metallic glasses – their rather limited room temperature ductility. An unique outcome of these studies is that the higher the number of intersecting shear bands with small shear offsets, the larger is the overall plastic deformation [1]. It has been suggested that shear banding localizes a large amount of shear strain in a very narrow planar band and results in softening due to disordering or heat generation [1,4,5]. When considering a network of intersecting shear bands, it is believed that the whole monolithic structure turns into a heterogeneous array of sheared and un-deformed regions which can result in a remarkable change in the macroscopic mechanical behavior of the BMGs [6–9]. The appearance of such heterogeneous structures in plastically deformed BMGs has been highlighted in terms of hardness gradients [10–13], residual strain/stress domains [9,14–20], and free volume changes [21,22]. These studies have well succeeded to draw a macroscopic image of a heterogeneous structure in BMGs. There have also been a limited number of computer simulations [23–25] and experimental studies [26–28] revealing the structural scale changes within or around shear bands. The measurement of the temperature profile along a shear band via in-situ thermographic observation [26,27] revealed that plastic

* Corresponding author. IFW Dresden, Institute for Complex Materials, P.O. Box 27 01 16, D-01171 Dresden, Germany.
*E-mail address:* h.shahabi@gmail.com (H. Shakur Shahabi).

http://dx.doi.org/10.1016/j.actamat.2016.03.035
1359-6454/

deformation can cause a very high temperature increase at the core of the shear band resulting in premature failure of the deforming BMG. Nano-indentation studies [28–30] at directions perpendicular to a shear band have identified a wide shear-induced region where the shear band has the lowest hardness and elastic modulus compared to other regions.

The above mentioned experimental studies had a spatial resolution of several microns and could not provide detailed knowledge on localized structural features like residual strains at the area around an individual shear band. To overcome this problem, we have performed a X-ray nano-beam diffraction study of single shear bands formed by cold-rolling of $Zr_{52.5}Ti_5Cu_{18}Ni_{14.5}Al_{10}$ (at.%) (Vit105) BMG. This enabled us to reveal the changes of the short- and medium-range atomic order in plastically deformed metallic glass on the nanoscale. For the first time, we have mapped fluctuations of the inter-atomic distances across and around a shear band and established that plastic deformation results in a strong residual elastic shear strain extending far beyond the localized region of shearing. It is shown that the magnitude and orientation of the residual shear strain trigger the nucleation of further shear bands.

### 1.1. Experimental details

Bulk metallic glass with nominal composition $Zr_{52.5}Ti_5Cu_{18}Ni_{14.5}Al_{10}$ (at.%) was prepared as a plate with a thickness of 1.4 mm and a width of 3 mm by centrifugal casting. The glassy plate was rolled in very small steps to reach a 5% of reduction in thickness. Before rolling, one transverse side of the plate was mirror-polished. After rolling, the plate was ground from the opposite side to a thickness of ~100 μm with twofold aim: i) to make it transparent for the nano-focused X-ray beam and ii) to have just one shear band on the X-ray passway. A detailed microstructure analysis of the cold-rolled and grounded plate using scanning electron microscope (SEM) proved presence of the shear bands and absence of cracks. An area of $25 \times 45\ \mu m^2$ with a single shear band was selected for the X-ray diffraction investigations and marked with platinum dots of about 5 μm size deposited by a Focused Ion Beam (FIB). These dots were found with a florescence detector and used as guide points to limit the area of the XRD scans. The X-ray beam had a wavelength of 0.189 Å and a size of 150 nm height and 5 μm width, measured as the full width at half maximum of a fluorescent peak from the deposited platinum dot. The selected area across a shear band was scanned with sample holder movements of 1.0 and 0.5 μ in the directions parallel and perpendicular to the shear band, respectively. The exposure time for each diffraction pattern was 5 s. A total number of 4538 diffraction patterns was recorded. The XRD patterns were integrated in 10° azimuthal slices between 0 and 360° with the Fit2D software [31]. The integrated data were processed using the PDFgetX3 package [32] to obtain the reduced pair distribution functions (PDF).

The position of the first shell in the structure function, $q_1$, was obtained by fitting to a Gaussian peak. In order to characterize the structural changes at SRO (Short Range Order) and MRO (Medium Range Order) scale in real space, the center of mass (CoM) of each coordination shell in the PDF was determined according to following equation:

$$CoM = \frac{\int_{root_{min}}^{root_{max}} rG(r)}{\int_{root_{min}}^{root_{max}} G(r)}, \quad (1)$$

in which G(r) represents reduced PDF, $root_{min}$ and $root_{max}$ indicate intersection of G(r) with the line G(r) = 0 at SRO region. The strain values, $\varepsilon^i$, for the different coordination shells were calculated according to the following equation:

$$\varepsilon^i_{deformed} = \frac{r^i_{deformed} - r^i_{undeformed}}{r^i_{undeformed}}, \quad (2)$$

where $r^i_{deformed}$ and $r^i_{undeformed}$ are the centers of mass of the $i$th shell in reduced PDF for a deformed and undeformed state, respectively. The scanned area in the cross section of this BMG includes regions between the shear bands which are far enough from two shear bands and thus are not affected by shearing. The peak positions of the diffraction patterns of several subsequent points in this region were the same. Thus the peak positions in the diffraction patterns of these points were chosen as the reference point to calculate the strain values. In order to calculate the components of the strain tensor, the angular variation of the strain, $\varepsilon^i_\theta$, was fitted to the following equation [33]:

$$\varepsilon^i_\theta = \varepsilon^i_x \cos^2\theta + \gamma^i_{xy} \cos\theta\sin\theta + \varepsilon^i_y \sin^2\theta, \quad (3)$$

where $\varepsilon^i_x$, $\varepsilon^i_y$ are the directions parallel and perpendicular to the shear band, respectively and $\gamma^i_{xy}$ is the in-plane shear strains. The maximum shear strain of each shell, $\gamma_{max}$, and its angle with the $x$ axis, $\theta_{\gamma max}$, were calculated according to the equations [34]:

$$\gamma_{max} = 2\sqrt{\left(\frac{\varepsilon_x - \varepsilon_y}{2}\right)^2 + \left(\frac{\gamma_{xy}}{2}\right)^2}, \quad (4)$$

$$\theta_{\gamma_{max}} = \theta_{\varepsilon_p} \pm 45^\circ, \quad (5)$$

where $\theta_{\varepsilon_p}$ is the principal strain angle, obtained via following equation [34]:

$$\tan 2\theta_{\varepsilon_p} = \frac{\gamma_{xy}}{\varepsilon_x - \varepsilon_y}, \quad (6)$$

## 2. Results and discussions

Fig. 1(a) presents a schematic of the X-ray diffraction investigations of the shear-zone in cold-rolled Vit105 bulk metallic glass. The rolled sample contains a sequence of parallel shear bands oriented at an angle of ±45° with respect to the rolling direction. The scanning electron microscopy (SEM) image in Fig. 1(b) shows a single shear band and a scanned area marked with a red rectangle. The X-ray intensities, as illustrated in Fig. 1(c), indicate a fully amorphous structure with no trace of crystallinity, implying that the studied region is free from deformation- or heating-induced crystallization.

It is known that the first maximum of the X-ray intensity or structure function taken from a metallic glass, and in particular the position of the first peak $q_1$, carries significant information on amorphous structure [35]. Recently, Poulsen et al. [36] showed that the components of the strain tensor in uniaxially deformed metallic glass can be determined from the positions of $q_1$ measured over all azimuthal directions with respect to the incident beam. We have determined the variation of the first peak on the XRD intensities over the whole scanned area across the shear band in cold-rolled Vit105 metallic glass. The corresponding maps for the fully integrated diffraction patterns and the XRD intensities measured in the planes along and perpendicular to the shear band are plotted in Fig. 2(a). The map of $q_1$ extracted from fully integrated patterns reveals an asymmetric gradient with respect to the shear band

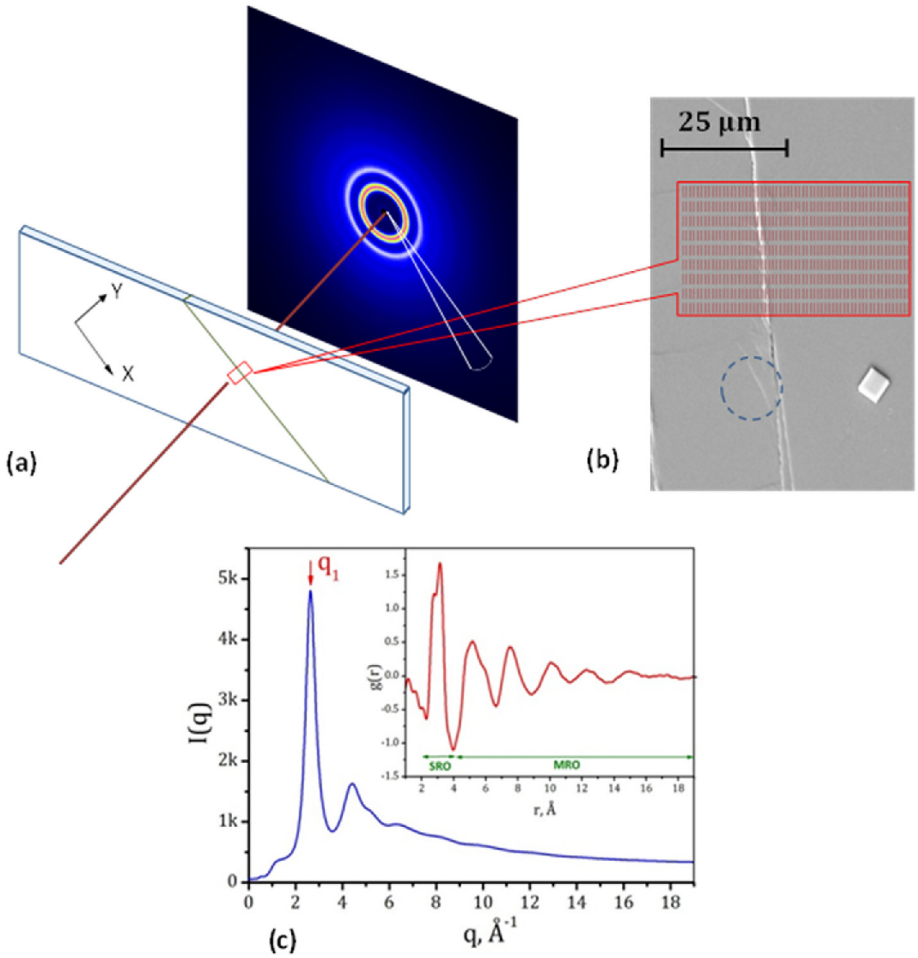


**Fig. 1.** Schematics of the sample and X-ray diffraction experiment (a) alignment of the beam, sample, and the two-dimensional detector; the *x* and *y*-axis were chosen parallel and perpendicular to the shear band. (b) Scanning electron microscopy (SEM) image of a studied single shear band; the blue circle marks a secondary shear band while the red rectangle depicts the scanned area. One of the four platinum markers deposited around the shear band is seen at the bottom-right; (c) Example of the integrated X-ray diffraction intensity versus wave vector (q) and reduced PDF (inset). (For interpretation of the references to color in this figure legend, the reader is referred to the web version of this article.)

plane which diversely affects the atomic structure in the area around the shear band. The maps of $q_1$ for the diffracted intensities at directions along and across the shear band in Fig. 2(b) and (c) represent more pronounced variations over the scanned area. This is a clear indication of a directional heterogeneity of the inter-atomic distances as a result of shear banding.

In order to obtain information on atomic distribution, one needs to transform the diffraction data from reciprocal space into real space, in which the peak positions represent inter-atomic distances [35]. Poulsen and co-workers [36] have shown on example of $Mg_{60}Cu_{30}Y_{10}$ BMG that the shift of peaks in the pair distribution function upon deformation represents the atomic scale strain. They observed that the strain at the low interatomic distances is significantly smaller than that at the larger scale [36]. In the case of multicomponent BMGs, it is difficult to determine the overall strain because of asymmetric shape of the maxima of pair distribution function g(r) caused by overlapping of several partial pair correlations. To overcome this problem, Hufnagel et al. [37] used the points in which $g(r) = 1$, arguing that the crossing point are less sensitive to the effects of asymmetry [38]. Alternatively, there have been studies [39–42] in which the center of mass of the first maximum in the pair distribution function was used to track structural changes upon mechanical or thermal actions. We have also observed that using of the center of mass of the first maximum results in considerably less scatter of the data compared to the positions of the individual sub-peaks.

Analysis of the pair distribution functions was performed along a line crossing the shear band, as indicated in Fig. 2(a). Fig. 3(a) and (b) present the profiles for the residual strains, $\varepsilon_x$, $\varepsilon_y$ and $\gamma_{max}$ determined from the first peak of the reduced PDF at about 2.9 Å, representing the nearest-neighbors shell, and from the fourth peak at about 10.1 Å, representing medium-range order. It is clearly seen that the residual strains spread over distances of more than 15 µm from the shear band. Together with the maps for $q_1$ in Fig. 2, this is surprisingly challenging the "localized" nature of the shear strain in a very narrow region (10–20 nm) of the shear band [1,4,5]. The so far reported experimental evidences of the shear-induced zone in Zr-based metallic glasses are related to the single shear bands with large shear offsets which are responsible for catastrophic failure of the sample [29,30]. In contrast, our current observations quantify the diffusive residual strain fields around a non-catastrophic mature shear band with small shear offset, formed during the plastic deformation of the metallic glass.

Similarly to the $q_1$ maps in Fig. 2, the normal strains indicate an asymmetric distribution with respect to the shear band line. According to Fig. 3(a) and (b), in the very vicinity of the shear band, the residual normal strains have opposite signs at the two sides of the shear band and the change from tensile to compressive strain

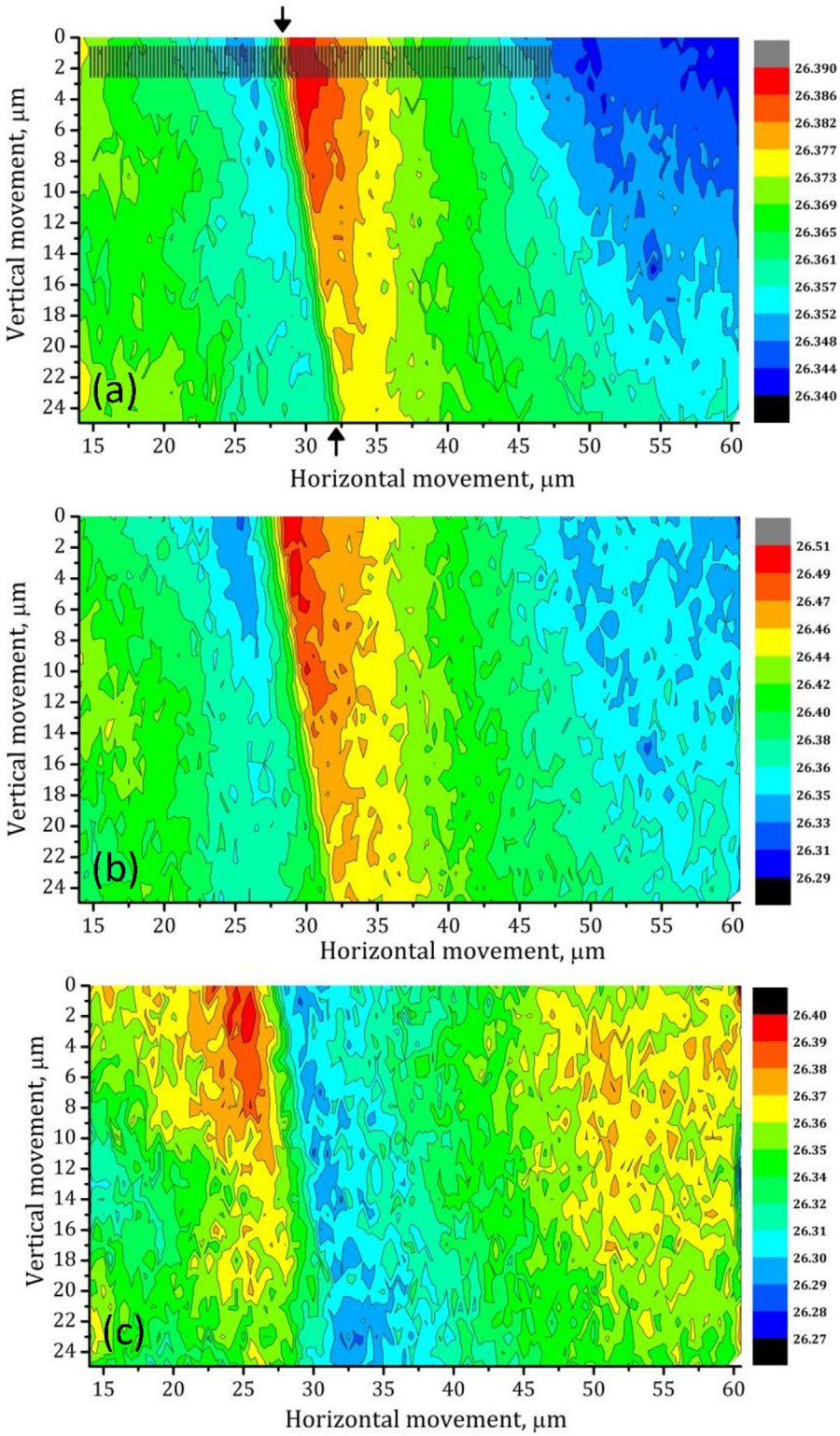


**Fig. 2.** Variation of the position of the first maximum of XRD intensities $q_1$ taken from the area containing a single shear band: (a) fully integrated diffraction patterns; (b) measured along the shear band; (c) measured perpendicular to the shear band. All three maps reveal that the atomic structure is essentially affected over rather large distances from the shear band. The arrows in panel (a) mark the shear band. The vertical lines across the shear band in panel (a) mark the area from which the data plotted in Fig. 3 were extracted.

occurs at the core of the shear band. The altered interatomic distances at $x$ and $y$ directions result in a residual shear strain component, $\gamma_{max}$, in the shear band and nearby regions. Contrary to the normal strains, $\gamma_{max}$ has a quasi-symmetric distribution with respect to the shear band with a maximum at the shear band and declining at farther distances. Such distribution of the residual shear strain is in good agreement with similar profiles of hardness [29,30] and elastic modulus [30] across a single shear band in Zr-

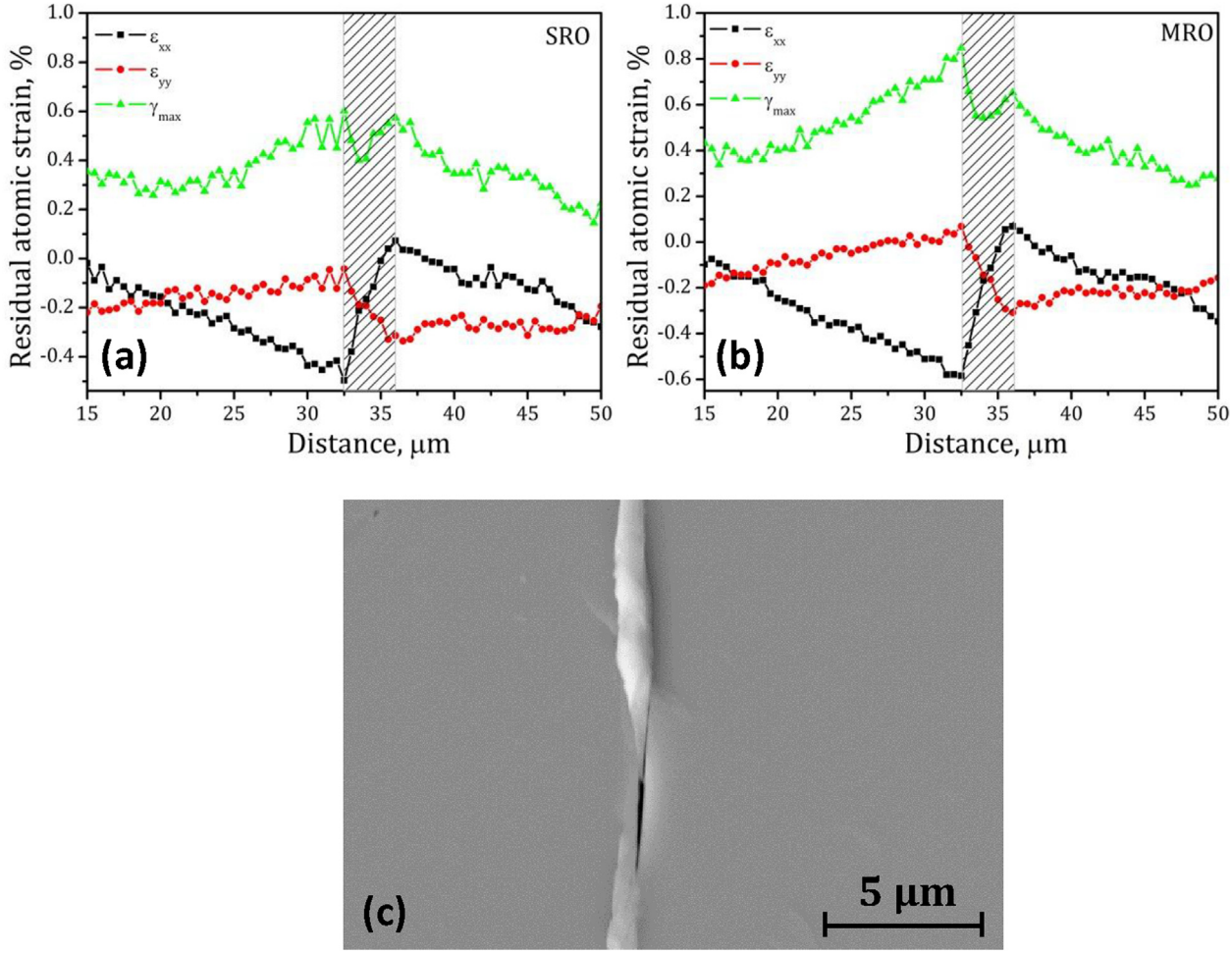


**Fig. 3.** Residual normal ($\varepsilon_x$ and $\varepsilon_y$) and maximum shear ($\gamma_{max}$) strain profile along the direction crossing the single shear band at (a) SRO, and (b) MRO, (c) The soft sheared material flows out of the shear band in the as-deformed BMG.

based BMGs. This suggests that compared to the residual normal strains, the residual shear strain field plays a dominant role in controlling the plastic deformation of the metallic glass. In addition, comparing the $\gamma_{max}$ values for the SRO and MRO (Fig. 3(a) and (b)) reveals that the residual strain is larger on the MRO distances. This is in agreement with the length scale dependence of the atomic strain in BMGs, as reported previously by others [38,43,44].

It is known that the maximum shear strain during deformation of bulk metallic glass is a crucial parameter in determining the nucleation of irreversible STZs [45]. As it is observed in Fig. 3(a) and (b), the magnitude of the shear strain at the vicinity of the shear band has the largest value when compared with the distances far from the core of the shear band. Although the shear strain around a single shear band has not been experimentally quantified so far, the fact that it has the highest value at the very vicinity of the shear band is expectable due to the nature of the shear in the core of the shear band. The more significant aspect of such kind of distribution is obtained by from the variation of maximum shear strain angle around the shear band. Fig. 4 shows the vectors of $\gamma_{max}$ calculated along the line crossing the shear band, as indicated in Fig. 2(a). The magnitude of the vectors is proportional to the absolute values of $\gamma_{max}$ while their directions are shown relative to the angle of $\gamma_{max}$. The direction of $\gamma_{max}$ in the shear band core (green shaded area) is parallel to the shear band for the short-range and medium-range interatomic distances. It is worth to note that when getting far from the center of the core region, the maximum shear strain direction deviates from the shear band plane and reaches an average angle of about ±24° at the border of the core region where the residual shear strain has its maximum value. This is in very good agreement with the direction of the observed secondary shear bands (Fig. 1(b)) which nucleate from the main shear band under an angle of ~25° with respect to the main shear band. In addition, a similar pattern of displacement vectors, obtained by molecular dynamics simulations, has been recently reported [24]. This proves the decisive role of the quantified residual shear strain in triggering the further plastic deformation of BMG via nucleation of new shear bands in the shear affected zone around a mature shear band.

The last but not least observation is a characteristic core region of about 3.5 μm width around the shear band (shaded rectangles in Fig. 3 (a) and 3(b)) which indicates an abrupt change in the normal strains. Correspondingly, $\gamma_{max}$ at both SRO and MRO exhibits a small local minimum in the middle of this region. A closer look at the SEM image with the shear band (Fig. 3 (c)) reveals material which has flown out of the shear band. This suggests that a necessarily soft amorphous region has been formed at the shear band during deformation. Together with the observed characteristic core zone for the residual strain fields, this is believed to represent the liquid-like/hot-zone region in a single shear band proved via melting of a thin tin layer by Lewandowski and Greer [46].

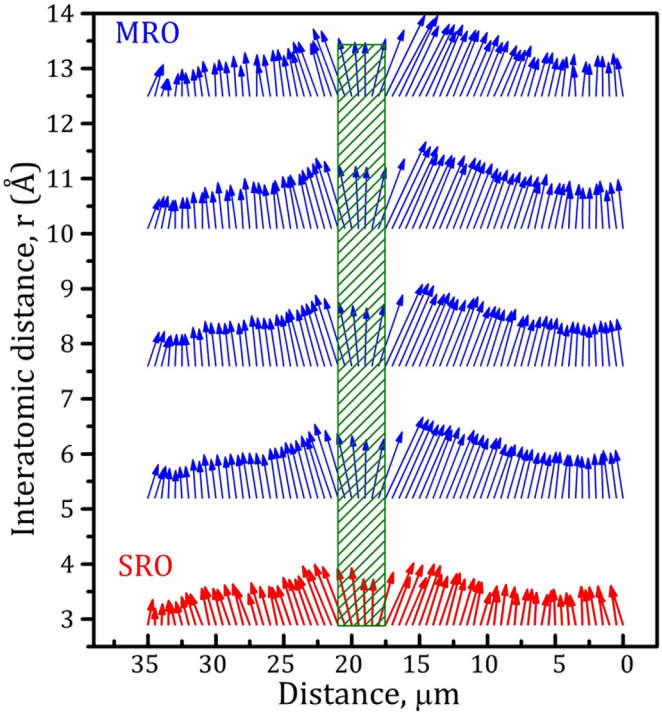


**Fig. 4.** Vectors of the residual maximum shear strain, $\gamma_{max}$, in and around a single shear band at different length scales (SRO and MRO) of the deformed BMG along the line crossing the shear band. The length of the vectors represents the relative magnitude of the shear strain.

To conclude our study, we demonstrated that the plastic deformation in cold-rolled $Zr_{52.5}Ti_5Cu_{18}Ni_{14.5}Al_{10}$ BMG results in diffusive residual normal and shear strain fields at both SRO and MRO length scale extending over distances more than 15 μm away from the shear band. The residual normal strains exhibit an asymmetric distribution whereas the residual shear strain is distributed symmetrically at the sides of the shear band. In agreement with reported distributions of elastic constants and hardness across a shear band, our results highlight the dominant role of the shear strain in governing further plastic deformation at regions near the shear band. This is also proved by the coincidence of the direction of the nucleating secondary shear bands from the main shear band with the orientation of the residual shear strain at the vicinity of the mature shear band.

## Acknowledgments

The authors thank D. Lohse, B. Sarac, C. Soyarslan, J. Wright, Z. Eskandari, M. Frey and S. Donath for technical assistance. The support from ESRF through the project No. HD/613 ID11, the German Science Foundation (DFG) under the Leibniz Program (grant EC 111/26-1) and Grant PA 2275/2-1, and the European Research Council under the ERC Advanced Grant INTELHYB (grant ERC-2013-ADG-340025) is gratefully acknowledged.

## References

[1] A.L. Greer, Y.Q. Cheng, E. Ma, Shear bands in metallic glasses, Mater. Sci. Eng. R Rep 74 (2013) 71–132.
[2] Y. Zhang, A.L. Greer, Thickness of shear bands in metallic glasses, Appl. Phys. Lett. 89 (2006).
[3] J. Kobata, T. Kimura, Y. Takigawa, T. Uesugi, H. Kimura, K. Higashi, Effect of pre-introduced shear bands direction on deformation behavior in Zr55Al10-Ni5Cu30 bulk metallic glass, Mater. Trans. 50 (2009) 2355–2358.
[4] W.J. Wright, M.W. Samale, T.C. Hufnagel, M.M. LeBlanc, J.N. Florando, Studies of shear band velocity using spatially and temporally resolved measurements of strain during quasistatic compression of a bulk metallic glass, Acta Mater. 57 (2009) 4639–4648.
[5] Y.Q. Cheng, Z. Han, Y. Li, E. Ma, Cold versus hot shear banding in bulk metallic glass, Phys. Rev. B 80 (2009).
[6] S. Scudino, B. Jerliu, S. Pauly, K.B. Surreddi, U. Kühn, J. Eckert, Ductile bulk metallic glasses produced through designed heterogeneities, Scr. Mater. 65 (2011) 815–818.
[7] S. Scudino, B. Jerliu, K.B. Surreddi, U. Kühn, J. Eckert, Effect of cold rolling on compressive and tensile mechanical properties of Zr(52.5)Ti(5)Cu(18)Ni(14.5)Al(10) bulk metallic glass, J. Alloy. Compd. 509 (2011) S128–S130.
[8] Q.P. Cao, J.W. Liu, K.J. Yang, F. Xu, Z.Q. Yao, A. Minkow, H.J. Fecht, J. Ivanisenko, L.Y. Chen, X.D. Wang, S.X. Qu, J.Z. Jiang, Effect of pre-existing shear bands on the tensile mechanical properties of a bulk metallic glass, Acta Mater. 58 (2010) 1276–1292.
[9] Y. Tong, W. Dmowski, Z. Witczak, C.P. Chuang, T. Egami, Residual elastic strain induced by equal channel angular pressing on bulk metallic glasses, Acta Mater. 61 (2013) 1204–1209.
[10] S. Scudino, K.B. Surreddi, M.S. Khoshkhoo, M. Sakaliyska, G. Wang, J. Eckert, Improved room temperature plasticity of Zr41.2Ti13.8Cu12.5Ni10Be22.5 bulk metallic glass by channel-die compression, Adv. Eng. Mater. 12 (2010) 1123–1126.
[11] L.Y. Chen, Q. Ge, S. Qu, J.Z. Jiang, Stress-induced softening and hardening in a bulk metallic glass, Scr. Mater. 59 (2008) 1210–1213.
[12] L. Wang, H. Bei, Y.F. Gao, Z.P. Lu, T.G. Nieh, Effect of residual stresses on the hardness of bulk metallic glasses, Acta Mater. 59 (2011) 2858–2864.
[13] K.K. Song, S. Pauly, Y. Zhang, S. Scudino, P. Gargarella, K.B. Surreddi, U. Kühn, J. Eckert, Significant tensile ductility induced by cold rolling in Cu(47.5)Zr(47.5)Al(5) bulk metallic glass, Intermetallics 19 (2011) 1394–1398.
[14] S. Scudino, H. Shakur Shahabi, M. Stoica, I. Kaban, B. Escher, U. Kühn, G.B.M. Vaughan, J. Eckert, Structural features of plastic deformation in bulk metallic glasses, Appl. Phys. Lett. 106 (2015) 031903.
[15] S. Yamanaka, K. Amiya, Y. Saotome, Effects of residual stress on elastic plastic behavior of metallic glass bolts formed by cold thread rolling, J. Mater. Process. Technol. 214 (2014) 2593–2599.
[16] F. Haag, D. Beitelschmidt, J. Eckert, K. Durst, Influences of residual stresses on the serrated flow in bulk metallic glass under elastostatic four-point bending - a nanoindentation and atomic force microscopy study, Acta Mater. 70 (2014) 188–197.
[17] Q. Wang, Y. Yang, H. Jiang, C.T. Liu, H.H. Ruan, J. Lu, Superior tensile ductility in bulk metallic glass with gradient amorphous structure, Sci. Rep. 4 (2014).
[18] Y. Zhang, W.H. Wang, A.L. Greer, Making metallic glasses plastic by control of residual stress, Nat. Mater 5 (2006) 857–860.
[19] F.O. Mear, G. Vaughan, A.R. Yavari, A.L. Greer, Residual-stress distribution in shot-peened metallic-glass plate, Philos. Mag. Lett. 88 (2008) 757–766.
[20] T.C. Hufnagel, U.K. Vempati, J.D. Almer, Crack-tip strain field mapping and the toughness of metallic glasses, PLoS One 8 (2013).
[21] A.R. Yavari, A. Le Moulec, A. Inoue, N. Nishiyama, N. Lupu, E. Matsubara, W.J. Botta, G. Vaughan, M. Di Michiel, A. Kvick, Excess free volume in metallic glasses measured by X-ray diffraction, Acta Mater. 53 (2005) 1611–1619.
[22] M. Stolpe, J.J. Kruzic, R. Busch, Evolution of shear bands, free volume and hardness during cold rolling of a Zr-based bulk metallic glass, Acta Mater. 64 (2014) 231–240.
[23] Y. Suzuki, T. Egami, Shear deformation of glassy metals: Breakdown of cauchy relationship and anelasticity, J. Non Cryst. Solids 75 (1985) 361–366.
[24] S. Feng, L. Qi, L. Wang, S. Pan, M. Ma, X. Zhang, G. Li, R. Liu, Atomic structure of shear bands in Cu64Zr36 metallic glasses studied by molecular dynamics simulations, Acta Mater. 95 (2015) 236–243.
[25] A. Tanguy, F. Leonforte, J.L. Barrat, Plastic response of a 2D Lennard-Jones amorphous solid: Detailed analysis of the local rearrangements at very slow strain rate, Eur. Phys. J. E 20 (2006) 355–364.
[26] W.H. Jiang, H.H. Liao, F.X. Liu, H. Choo, P.K. Liaw, Rate-dependent temperature increases in shear bands of a bulk-metallic glass, Metall. Mater. Trans. A Phys. Metall. Mater. Sci. 39A (2008) 1822–1830.
[27] B. Yang, P.K. Liaw, G. Wang, M. Morrison, C.T. Liu, R.A. Buchanan, Y. Yokoyama, In-situ thermographic observation of mechanical damage in bulk-metallic glasses during fatigue and tensile experiments, Intermetallics 12 (2004) 1265–1274.
[28] R. Maaß, P. Birckigt, C. Borchers, K. Samwer, C.A. Volkert, Long range stress fields and cavitation along a shear band in a metallic glass: The local origin of fracture, Acta Mater. 98 (2015) 94–102.
[29] J. Pan, Q. Chen, L. Liu, Y. Li, Softening and dilatation in a single shear band, Acta Mater. 59 (2011) 5146–5158.
[30] R. Maaß, K. Samwer, W. Arnold, C.A. Volkert, A single shear band in a metallic glass: Local core and wide soft zone, Appl. Phys. Lett. 105 (2014).
[31] A.P. Hammersley, S.O. Svensson, M. Hanfland, A.N. Fitch, D. Hausermann, Two-dimensional detector software: from real detector to idealised image or two-theta scan, High. Press. Res. 14 (1996) 235–248.
[32] P. Juhas, T. Davis, C.L. Farrow, S.J.L. Billinge, PDFgetX3: a rapid and highly automatable program for processing powder diffraction data into total scattering pair distribution functions, J. Appl. Crystallogr. 46 (2013) 560–566.
[33] G. Ellwood Dieter, Mechanical Metallurgy, McGraw-Hill, 1976.
[34] S. Timoshenko, J.M. Gere, Mechanics of Materials, Van Nostrand Reinhold Co., 1972.
[35] B.E. Warren, X-ray Diffraction, Dover Publications Inc., New York, 1990.

[36] H.F. Poulsen, J.A. Wert, J. Neuefeind, V. Honkimaki, M. Daymond, Measuring strain distributions in amorphous materials, Nat. Mater. 4 (2005) 33–36.
[37] U.K. Vempati, P.K. Valavala, M.L. Falk, J. Almer, T.C. Hufnagel, Length-scale dependence of elastic strain from scattering measurements in metallic glasses, Phys. Rev. B 85 (2012) 214201.
[38] T.C. Hufnagel, R.T. Ott, J. Almer, Structural aspects of elastic deformation of a metallic glass, Phys. Rev. B 73 (2006) 064204.
[39] T. Wilson, B. Clausen, T. Proffen, J. Elle, D. Brown, In-situ neutron scattering measurement of stress-strain behavior of a bulk metallic glass, Metall. Mater. Trans. A-Phys. Metall. Mater. Sci. 39A (2008) 1942–1946.
[40] K. Georgarakis, D.V. Louzguine-Luzgin, J. Antonowicz, G. Vaughan, A.R. Yavari, T. Egami, A. Inoue, Variations in atomic structural features of a supercooled Pd–Ni–Cu–P glass forming liquid during in situ vitrification, Acta Mater. 59 (2011) 708–716.
[41] J. Bednarcik, S. Michalik, M. Sikorski, C. Curfs, X.D. Wang, J.Z. Jiang, H. Franz, Thermal expansion of a La-based bulk metallic glass: insight from in situ high-energy x-ray diffraction, J. Phys. Condens. Matter. 23 (2011) 254204.
[42] H. Lou, X. Wang, Q. Cao, D. Zhang, J. Zhang, T. Hu, H.-k. Mao, J.-Z. Jiang, Negative expansions of interatomic distances in metallic melts, Proc. Natl. Acad. Sci. 110 (2013) 10068–10072.
[43] Y. Suzuki, J. Haimovich, T. Egami, Bond-orientational anisotropy in metallic glasses observed by x-ray-diffraction, Phys. Rev. B 35 (1987) 2162–2168.
[44] H.S. Shahabi, S. Scudino, I. Kaban, M. Stoica, U. Rütt, U. Kühn, J. Eckert, Structural aspects of elasto-plastic deformation of a Zr-based bulk metallic glass under uniaxial compression, Acta Mater. 95 (2015) 30–36.
[45] W.L. Johnson, K. Samwer, A universal criterion for plastic yielding of metallic glasses with a (T/T-g)(2/3) temperature dependence, Phys. Rev. Lett. 95 (2005) 195501.
[46] J.J. Lewandowski, A.L. Greer, Temperature rise at shear bands in metallic glasses, Nat. Mater 5 (2006) 15–18.